Thermochimica Acta, 226 (1993) 85–98
Elsevier Science Publishers B.V., Amsterdam

Structure and properties of ultralow density polyethylenes [1]

L. Woo *, Stanley Westphal and T.K. Ling
Baxter Healthcare, Round Lake, IL 60073-0490 (USA)

(Received 29 September 1992; accepted 19 April 1993)

Abstract

With new advances in catalyst technology, polyethylenes of unprecedented lower densities are rapidly being introduced. Because these very low density polyethylenes offer very interesting mechanical properties, a systematic investigation into their thermal and mechanical properties has been made. It was found, for example, that despite the low densities achieved, wide compositional variations existed berween materials. A comparison was also made between the thermal and mechanical properties and the optical properties, with the conclusion that compositional homogeneities are required for good optical properties.

INTRODUCTION

Ever since the Zeigler–Natta synthesis of polyolefins, there has been a desire to create progressively lower density materials by copolymerization. These lower density olefins potentially offer a range of attractive properties such as lower moduli (higher flexibility), greater toughness and lower heat-seal initiation temperatures. Until recently, the lowest density which was commercially achievable remained near the 0.915 range. However, in the last few years new catalysts, coupled with improved processes, have resulted in a large number of claims for products of ever-decreasing densities and various properties.

In the medical industry, these lower density olefins present certain very interesting possibilities for product designs. Therefore, we have undertaken a systematic study of the relationships between the thermal and mechanical properties, and the structural and compositional parameters to gain some insight into the key parameters controlling performance. The samples included in the study are:

* Corresponding author.

[1] Presented in part at the 21st Annual NATAS Conference, Atlanta, GA, 13–16 September 1992.

(i) Tafmer A-4085 (Mitsui Petrochemical), ethylene butene solution process copolymer.
(ii) Flexomer 1210 (Union Carbide), ethylene butene copolymer from the Unipol® gas-phase process.
(iii) Attane 4002 (Dow Chemical), octene copolymer from a solution process.
(iv) Exact 4024 (Exxon), ethylene butene copolymer from a high-pressure process.

Analysis of the Tafmer by ^{13}C-NMR indicated that it contained about 16 wt.% butene [1]. The Exxon material was produced using a single-site catalyst and a metallocene as the coordination ligand. In addition, 18 wt.% and 28 wt.% ethylene vinyl acetate (EVA) copolymers produced by the high-pressure process were used for comparison. A description of the basic properties obtained from the resin manufacturers is given in Table 1.

TABLE 1
Material designations

Sample	Grade	Density/ g cm^{-3}	Melt index/ g per 10 min
A	Tafmer A-4085	0.88	3.6
B	Exact-4024	0.88	2.2
C	Attane-4002	0.912	3.3
D	Flexomer DEFD-1210	0.89	1.0
E	18% EVA	0.94	0.45
F	28% EVA	0.95	3.2

EXPERIMENTAL

Samples were first compression-molded into approx. 0.2-mm-thick films on a compression molding press at 190°C. Thermal properties were measured on a TA Instruments 2910 differential scanning calorimeter (DSC) cell using a model 2100 controller. Heating and cooling rates of 10°C min^{-1} and 5°C min^{-1}, respectively, were used throughout this study. A Seiko dynamic mechanical analyser (DMA) DMS-110 was used for wide frequency range (0.5–100 Hz) studies over the temperature range of −150–150°C. Rheological data were collected over broad temperature ranges using a Rheometrics RFR rheometer with parallel-plate geometry in the dynamic mode, over frequencies of 0.1–300 radians s^{-1}. Mechanical properties were measured on an MTS 8100 servohydraulic tester at 50–500 cm min^{-1} crosshead velocity. Strain recovery experiments were conducted by first elongating the samples to 25% strain, and then the

percentage recovery upon removal of the stress was measured. Cyclic creep was measured as the increased sample dimension after 1000 cycles at 70% strain. Optical haze measurements were taken on a Hunter colorimeter according to ASTM D-1003. In order to eliminate haze contribution from surface imperfections, both film surfaces were wetted with isopropanol. In this way, only the internal haze from the material was measured. Scanning electron microscopy (SEM) was carried out on palladium-coated samples on either a JEOL 6300F or a JEOL 35CF instrument. In addition, other available characterization data were incorporated into this study.

RESULTS AND DISCUSSION

Thermal and mechanical properties

The second-heat thermal data are shown in Table 2; the mechanical property data are presented in Table 3.

There is a clear relationship between the tensile modulus (Young's modulus) and the crystallinity [2] or the 1-Hz dynamic elastic modulus and

TABLE 2

Thermal analysis data

Sample	T_m/°C	Heat of fusion/ J g^{-1}	% Crystallinity [a]
A	69.5	59.8	20.4
B	71.8	62.0	21.2
C	123.8	125.6	42.9
D	118.4	74.8	25.6
E	84.1	74.8	25.6
F	69.9	60.3	20.6

[a] 292 J g^{-1} was taken as the 100% crystalline polyethylene [2].

TABLE 3

Mechanical properties

Sample	Tensile modulus/ 10^7 Pa	1 Hz dynamic modulus/ 10^7 Pa	Strain recovery in %	Creep in %
A	3	3.8	95	22
B	2.5	3.5	98	24
C	15	31	63	71
D	5.7	8	74	59
E	4.5	5.5	83	36
F	1.6	1.6	92	23

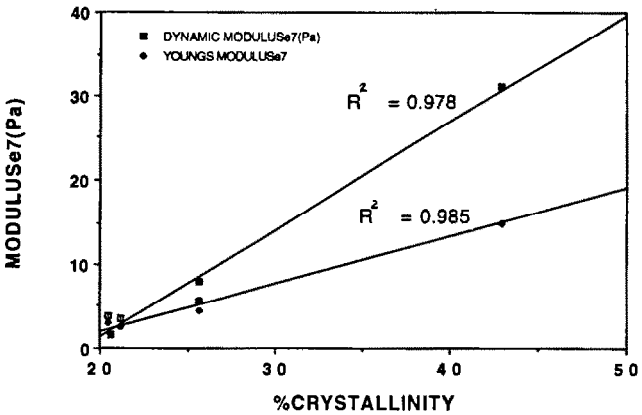

Fig. 1. Moduli versus crystallinity of the samples.

the crystallinity (Fig. 1). Furthermore, there is also a good correlation between the strain recovery at 25% strain and the crystallinity (Fig. 2). The nearly constant ratio of the dynamic elastic modulus compared with the tensile modulus can be attributed to the typical strain-softening of the materials. Therefore data from the DMA at strains much lower than 1% are expected to be higher than the tensile modulus measured at finite, approx. 2–5%, strains. Of course, another separate contribution to this systematic deviation is the time-scale dependence of the moduli being measured.

However, the melting temperature of the polymers was not found to be a unique function of the crystallinity. Nor was the cyclic creep a unique function of the crystallinity. This was shown in Figs. 3 and 4. These

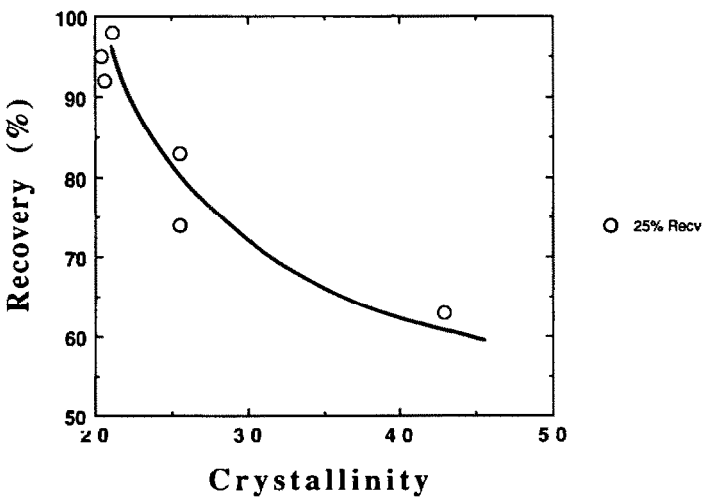

Fig. 2. Strain recovery versus crystallinity (25% initial strain).

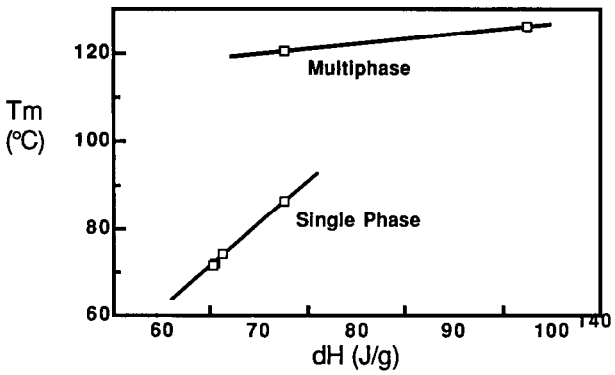

Fig. 3. Peak melting point versus crystallinity.

functional dependences suggest that there are two separate families, or classes, of materials describing the resin behavior.

The distinction between the two groups of polymers is compositional heterogeneity. This is illustrated in the DSC melting curves. The melting temperature of a copolymer is a function of the amount of comonomer incorporated into the crystallizing chain [3]. If the comonomer incorporation is neither random nor uniform in each chain, then multiple melting peaks would be anticipated which are characteristic of a particular copolymer species. This behavior is illustrated in Fig. 5. The DSC melting curves of samples C and D both exhibit multiple melting peaks. The melting behavior of the other materials is that of a single melting species.

A more direct way to quantify this heterogeneity is using temperature rising elution fractionation (TREF) [4] in which molecules are separated according to their crystallizability. The most highly branched polyethylene molecules are the least crystallizable and are recovered first in the experiment. This procedure was carried out on samples A, C and D. The compositional distributions of these materials are shown in Fig. 6. These

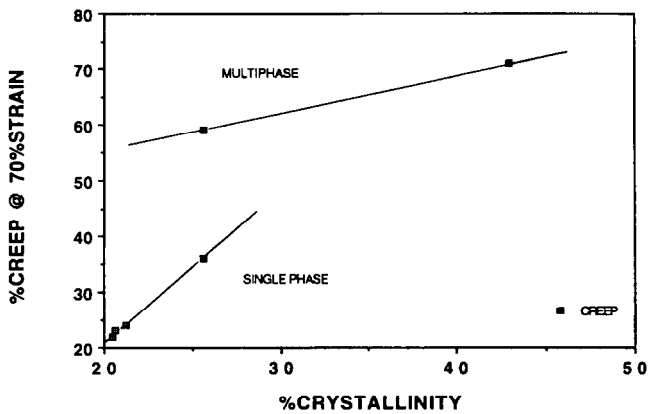

Fig. 4. Cyclic creep versus crystallinity (1000 cycles, 70% strain).

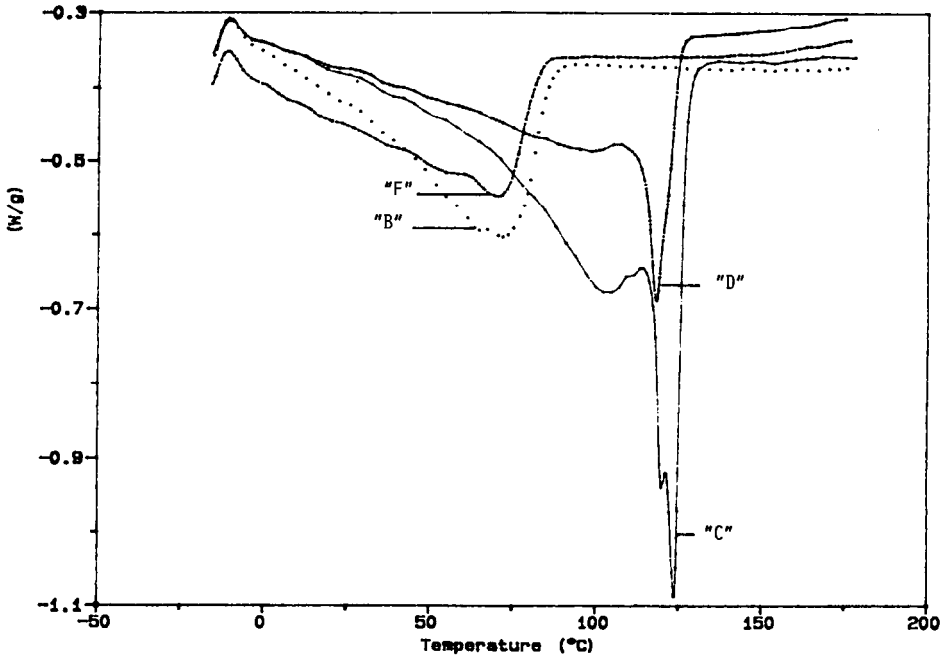

Fig. 5. DSC melting endotherms (5°C min^{-1}).

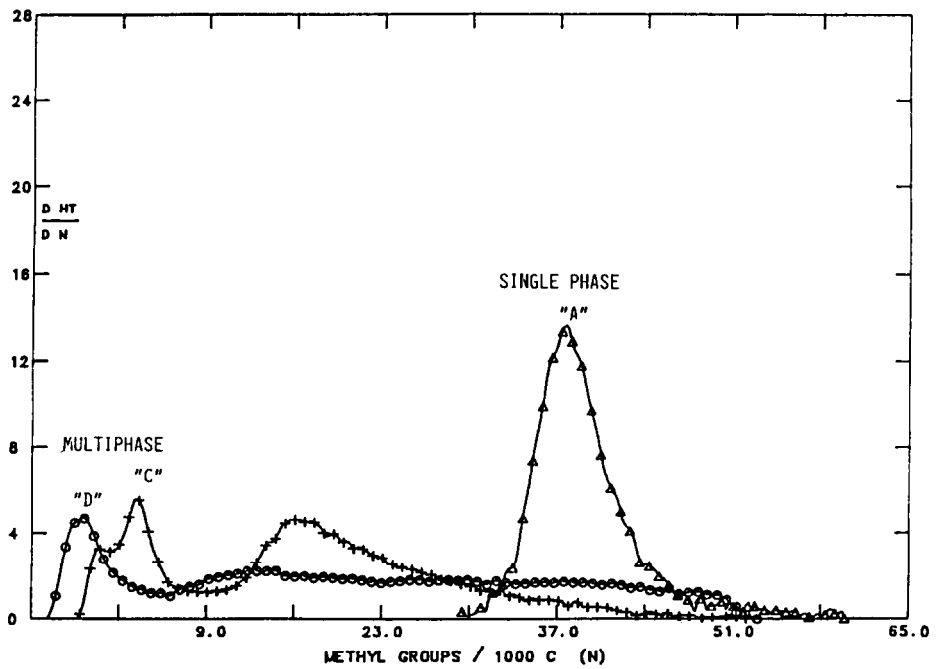

Fig. 6. Short chain branching distributions by TREF.

results indicate that the composition of sample A is much narrower than the compositions of samples C and D. These two samples contain materials which range from linear and highly crystallizable components to components that are highly branched and amorphous. This is mirrored qualitatively in the DSC melting curves. Morphological studies on similar types of polyethylenes by one of the authors have shown that the broad-composition polymers exist as multiphase materials [5]. Other studies have shown that the molecular weight of the most highly branched materials is lower than the bulk in similar broad-composition copolymers [6].

From data presented in this study, we can conclude that samples C and D are also multiphase polymers. The observed two distinct classes of responses arise primarily from this structural heterogeneity.

Dynamic mechanical properties

The dynamic mechanical spectra were quite interesting and deserve further comment. The elastic moduli and tan δ at 1 Hz are presented in Figs. 7 and 8. Comparing the elastic moduli as a function of temperature, one sees that all samples reach a low-temperature plateau of about 5 GPa,

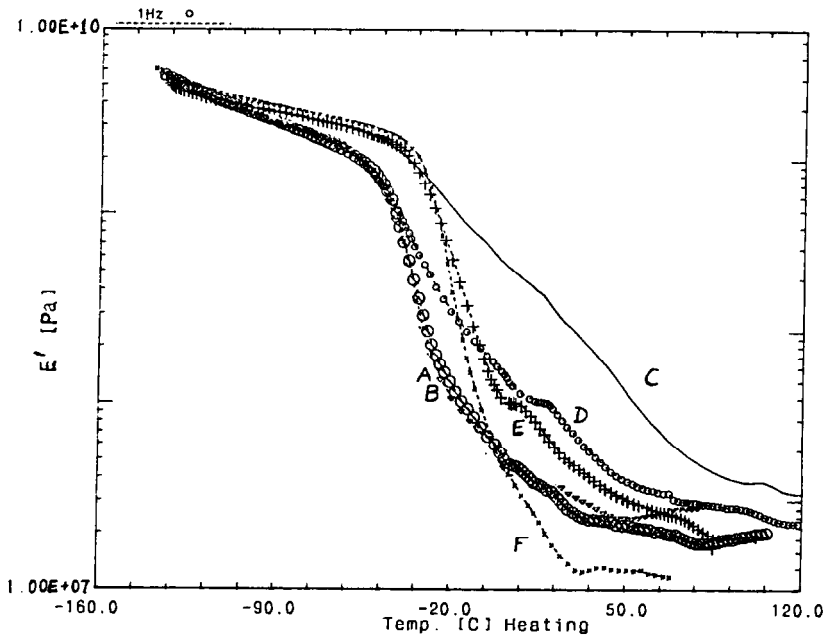

Fig. 7. DMA elastic moduli (1 Hz) over temperature.

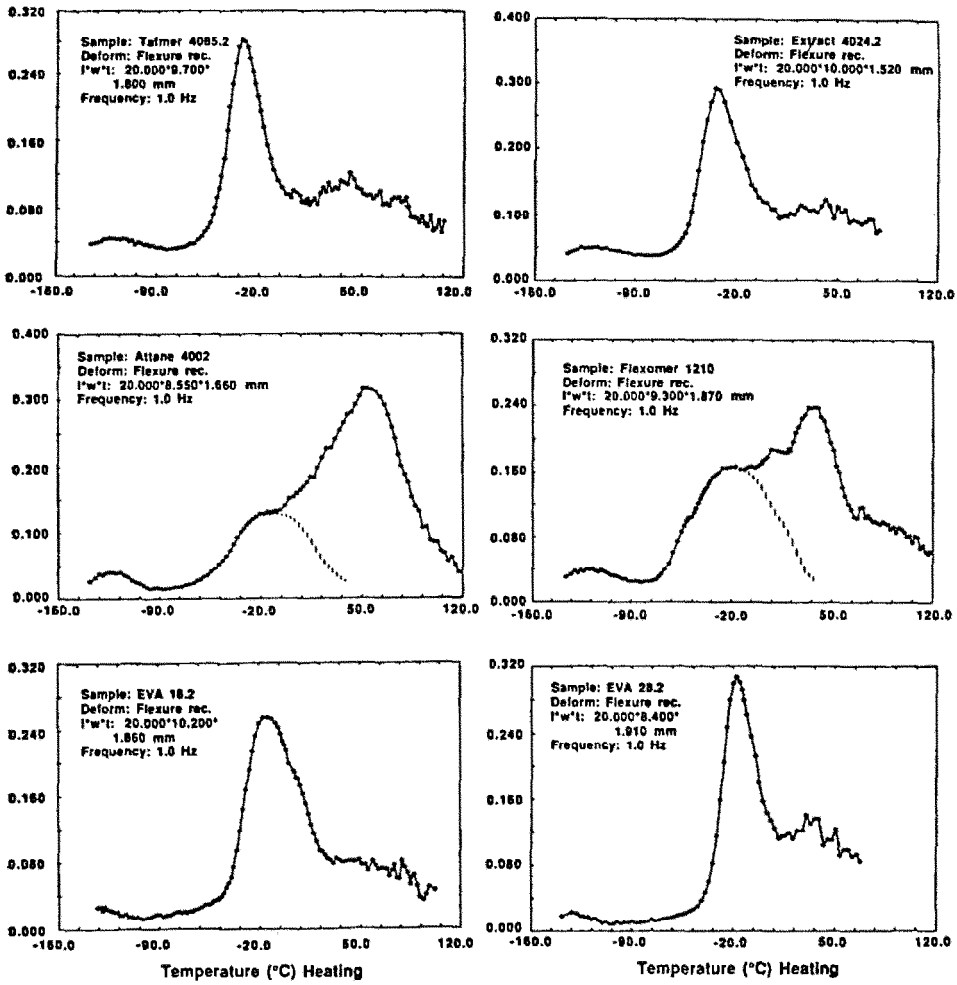

Fig. 8. DMA loss tangent (1 Hz) versus temperature.

in agreement with the glassy plateau limiting modulus exhibited by most polymers. On passing through the γ-transition normally attributed to the so-called "crank-shaft" motion of the methylene sequences of greater than three carbons at about −120°C, the moduli were reduced to about 2 GPa, before the onset of the next major transition at about −50°C. The second transition is the β-transition normally assigned to the relaxation of the tertiary carbon at the branch point for the side groups. In our samples, these are the ethyl branches for butene comonomers, hexyl branches for octene copolymers, and acetate side-groups for the vinyl acetate copolymers. The type, number and distribution of these branches appear to influence the location and the modulus reduction at the β-transition. For samples A and B, a rather steep decrease in the elastic modulus is seen before the sample reaches −30°C, while the modulus decreases to less than

0.1 GPa. Equally drastic reductions in elastic moduli are also seen in samples E and F (EVAs), although starting at a somewhat higher temperature. The higher VA-content sample, F, underwent the steepest modulus reduction to about 30 MPa at −5°C. In the region between 0 and 50°C, and before the melting point of the materials, the reinforcing effect of the crystalline phase becomes evident. In the low crystallinity samples A, B, E and F, a slight shoulder can be seen on the elastic modulus. For the higher crystallinity sample C, due to the lower number of branches, the elastic modulus was only reduced to about 0.7 GPa at 0°C. For sample C, a very broad, gradual reduction in modulus was evident starting at about −65°C, extending to about 50°C, with several detectable changes of slope between these two temperatures.

Comparing the loss tan δ, over the temperature range, all samples exhibit the typical three relaxation peaks: the γ-transition at about −120°C, the β-relaxation at about −30 to −20°C, and the α-transition between 0°C and the final melting point of the samples. The α-transition is usually assigned to relaxations in the crystalline domain [7]; therefore it is not surprising that its observed magnitude in our samples is strongly dependent on crystallinity. In the higher heterogeneous sample D, resolvable transitions to normally assigned [7] α and α' components were clearly evident.

Because our samples differ considerably in comonomer content and type, the β-relaxation supplies the most interesting comparison. First, we observed that the alkyl-branched samples A, B, C and D, exhibited a linear dependence (Fig. 9) of the β-transition temperature with the peak melting point. When the melting peak is extrapolated to 140°C, the melting point for homopolymers, the β-transition is located at about −10°C, in

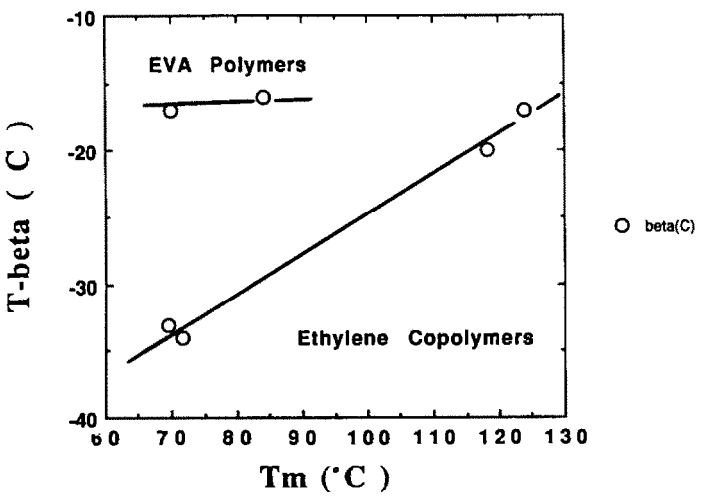

Fig. 9. β-Transition temperatures versus peak melting temperature.

TABLE 4
β-Transition

Sample	β-Peak/°C	β-FWHH/°C
A	−33	25.2
B	−34	26
C	−17	53
D	−20	76
E	−16	43
F	−17	26

reasonable agreement with the value near 0°C observed by Flocke [8] with quenched HDPE at 3 Hz. At present, there is no clear explanation as to why sample D, with extensive structural heterogeneity, should follow the same relationship displayed by its much more homogeneous counterparts.

The more polar and, presumably, more randomly distributed acetate branches appeared to exhibit a nearly constant transition temperature at about −20°C, in agreement with data reported in the literature [9]. Also, becuase the β-relaxation originated from the region of the main chain near the tertiary carbon at the branch points, the width of the relaxation process offers an indication of the "type" and number of these branch points, i.e., the homogeneity of the branch distribution. The width of the β-transitions, as measured by full width half-heights (FWHH), are compared with the optical haze, a very sensitive measure of the homogeneity of the components, in Fig. 10.

Yet another indication of the structural heterogeneity is the relatively high tan δ values for samples C and D at ambient temperatures. At 25°C,

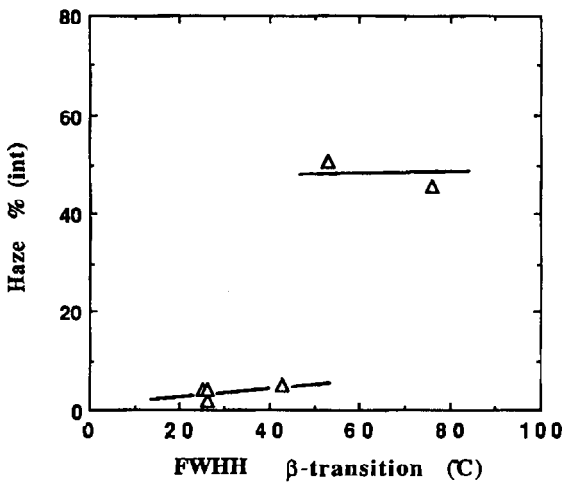

Fig. 10. Optical haze versus β-transition line width (FWHH).

this is in the vicinity of the polyethylene α-transition. The α-transition is commonly assumed [8] to originated from chain reorientation motions in the crystalline domain. For sample C, the higher $\tan\delta$ can simply be attributed to the higher crystallinity. However, for sample D, whose crystallinity is quite low, the greater mechanical loss must arise from a different origin. A most likely explanation is that "liquid-like" domains existed and were trapped in the crystalline phase. These liquid-like domains are the products of low molecular weight oligomers during the polymerization reaction. Upon storage at ambient temperature for about a week after the fabrication process, a viscous oil-like substance was observed to migrate to the surface. This observation is consistent with the low molecular weight liquid domain hypothesis.

Optical properties

The measured internal optical haze of the sample films of about 125 μm in thickness are presented in Table 5.

For the optical properties, for particle sizes below 1–5 μm, the turbidity is described by the Rayleigh–Gans equation [10]

$$\tau = 8/9(2\pi/\lambda)^4(\mu_2/\mu_1 - 1)^2R^3\phi \quad (1)$$

where ϕ is the volume fraction of the second phase, λ is the wavelength, μ the refractive indices of the matrix (1) and the particles (2), and R the radius of the particles.

From eqn. (1), the turbidity should be proportional to the volume fraction of the crystalline phase or roughly to the crystallinity, and highly dependent on the presence of larger size particles in the 1–5 μm range due to the third-power dependence.

Figure 11 presents the optical haze measurements plotted against crystallinity. Two disconnected lines each with a slight dependence on crystallinity were obtained, with a gap of more than 40% haze units

TABLE 5

Internal optical haze (sample thickness approx. 125 μm) [a]

Sample	Haze in %
A	4
B	4
C	51
D	46
E	5
F	2

[a] Haze measured according to ASTM D-1003.

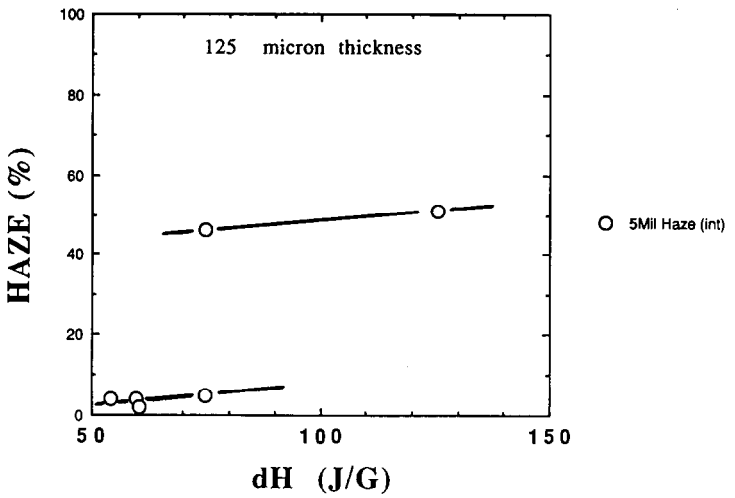

Fig. 11. Optical haze versus heat of fusion.

separating the two families. Undoubtedly, at higher crystallinities, the crystallite size and the optical scattering centers grew larger, and from the power-law dependence, greatly contributed to the observed high turbidity. However, sample D presented an anomaly. Its crystallinity is nearly identical to that of sample E, the EVA with 18% VA content, and yet the measured haze is about an order of magnitude higher. The only reasonable explanation is that the sample is very heterogeneous, with its crystallinity distributed among scattering centers of vastly different sizes. To gain a better understanding, the melting endotherms of Fig. 5 are replotted in integral form in Fig. 12. In addition, if we assume that the melted fraction at a given temperature is proportional to the crystallite size [11], it can immediately be seen that the higher melting (larger size) fractions have a

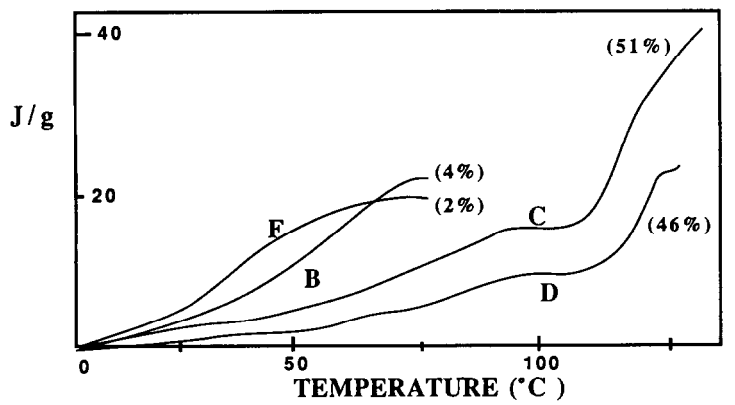

Fig. 12. DSC melting, enthalpy of fusion versus temperature. Numbers in parentheses are measured internal haze of 125-μm films.

disproportionate contribution to the optical haze from the third-power dependence. From this discussion, one can conclude that for good optical properties, not only does the crystallinity need to be low, but also the branching distribution needs to be very homogeneous to minimize the high scattering from the higher melting and larger size crystallites. As discussed in the dynamic mechanical section, the width of the β-relaxation as measured in the full width at half height (FWHH) is a sensitive measure of the type and number distribution of the branches. This method could potentially provide insight into the structures of these polymers, or at least, be a complimentary technique to TREF. It is also interesting to note that the DMA β-relaxation strength (height of the peak) and location (temperature and frequency of activation) is a direct spectroscopic measure of the chain dynamics near the branch points, while the TREF technique measures the effect of branching on crystallizability.

The high mechanical loss and creep may be explained by the low molecular weight (low strength) amorphous and liquid-like domains forming networks that are mechanically connected with the overall structure. These weak sections are easily deformed and flow under stress, and, due to their low molecular weight, are unable to form entanglements for the creation of restoring forces, thus retaining the deformation as creep or permanent set. Further work to integrate this model into actual morphologies is currently in progress.

CONCLUSIONS

We have examined a series of commercially available very low density and ultralow density polyethylenes. In addition to the crystallinity, the structural homogeneity as measured by the comonomer distribution was found to be very important for many of the mechanical and optical properties. This comonomer distribution can be measured by TREF. The deviation of the peak melting point from the density relationship, or the presence of multiple melting peaks, and the width of the β-relaxation in the dynamic mechanical spectra are separate evidences of the structural inhomogeneity.

ACKNOWLEDGEMENTS

^{13}C-NMR data from T. Bouton and TREF data from L. Wild are gratefully acknowledged.

REFERENCES AND NOTES

1 T. Bouton, private communications.
2 The value of 292 J g^{-1} was taken as the 100% crystalline polyethylene, see B. Wundelich, Macromolecular Physics, Vol. 1, Academic Press, New York, 1973, p. 388.
3 P.J. Flory, J. Chem. Phys., 17 (1949) 223.

4 L. Wild, T.R. Ryle, D.C. Knobeloch and I.R. Peat, J. Polym. Sci. Polym. Phys. Ed., 20 (1982) 441.
5 F. Mirabella and S. Westphal, P.L. Fernando, E.A. Ford and J.G. Williams, J. Polym. Sci. Polym. Phys. Ed., 26 (1988) 1995.
6 T. Usami, Y. Gotah and S. Takayama, Macromolecules, 19 (1986) 2722.
7 I.M. Ward, Mechanical Properties of Solid Polymers, Wiley, New York, 2nd edn., 1983.
8 H.A. Flocke, Kolloid Z., 180 (1962) 118.
9 L. Nielson, J. Polym. Sci., 42 (1960) 357.
10 C.B. Bucknall, Toughened Plastics, Applied Science, London, 1977.
11 J. Mack, A. Eisenberg, W. Graessley, L. Mandelkern and J. Koenig, Physical Properties of Polymers, ACS, Washington DC, 1984.